16TH EUROPEAN CONFERENCE ON EARTHQUAKE ENGINEERING THESSALONIKI 18 - 21 JUNE 2018

MODAL CHARACTERIZATION OF STRUCTURE AND SOIL-STRUCTURE INTERACTION USING ACCELEROMETRIC DATA OF THE FRENCH PERMANENT NETWORK (RAP-RESIF): APPLICATION TO A FRENCH INDIES STRUCTURE IN BASSE-POINTE, MARTINIQUE

Julie REGNIER[1], Anne DUCHEZ[2], Nathalie DUFOUR[3] and Philippe GUEGUEN[4]

ABSTRACT

In the scope of seismic risk mitigation, a high school in French Indies was instrumented with accelerometric sensors in 2014. We lead and extensive analysis of the data recorded both earthquake and ambient vibrations. The analysis provides a modal characterization of the structure, the earthquake and noise recordings provide close results but the first longitudinal mode frequency differs which may indicate that earthquake data could trigger modes that are not seen by ambient vibration especially rocking of the foundations. Frequencies and modes shapes were used to up-date a numerical simulation of the building to be able to provide the dynamic behavior of the structure during strong ground motion. The comparison between observations and prediction indicate that the non-structural elements must be considered when compared to weak motion data.

Accelerometric data ; modal analysis ; soil-structure interaction

1. INTRODUCTION

Martinique island, located in the French Indies, is in the French territory that is the most subject to earthquake hazard. The French government led an initiative to reduce the vulnerability of public building and especially schools of French Indies. In this context, the French accelerometric network (RAP/RESIF) instrumented permanently a high school located at Basse-Pointe. After six years of earthquakes and ambient vibrations recordings, a rich accelerometric database is now available.

In this project, we want to get one step further and to develop a modelling of the dynamic behavior of the structure during strong earthquakes. To do so, we create a numerical modelling without soil structure interaction to calibrate the parameters of the structure with weak motion data. However, such task is not straight-forward as the data contain the whole soil-foundation-structure system response while only part of the system answer will be modelled.

Methods have been developed to identify modal parameters of each part of the system considering soil-structure interactions, lateral and rocking movement of the foundations (e.g. Chandra, 2014 ; Stewart et Fenves, 1998 ; Todorovska, 2009a ; Todorovska, 2009b). For this analysis, a specific instrumentation of the structure is required and available at the high school in Basse-Pointe (Martinique).
The objective of this study is to use earthquake and noise recordings to assess the dynamic behavior of a soil-foundation-structure system and to figure the behavior of each part of the system such that the

[1] Phd, Project-team MouvGS, Cerema, Sophia-Antipolis, France, julie.regnier@cerema.fr
[2] Ingineer, DREC, Cerema, Aix-en-Provence, anne.duchez@cerema.fr
[3] Phd, Project-team MouvGS, Cerema, Aix-en-Provence, France, nathalie.dufour@cerema.fr
[4] Phd, ISTerre-IFSTTAR, Grenoble, France, philippe.gueguen@cerema.fr

numerical modelling of the seismic response of the structure can be improved. First, the building is presented with the instrumentation that has been permanently installed by the RAP/RESIF French accelerometric network. Then, the earthquakes database is illustrated and the frequency analysis that were performed for the modal identification is shown. Finally, a comparison between the results of the numerical simulation of the building and the in-situ measurement is shown to improve the building modelling.

2. CASE OF STUDY

The building considered in this study is a high school located at Basse-Pointe (CGBP) and built in the 1970's. This is a 3-story building made of two parts, called east and west parts, and separated by a 4 cm expansion joint. The dimensions of the building are about 9 m by 57 m with story heights of 3 m. An overview of the building and the first floor plan view are presented in Figure 1.
The structural system is reinforced concrete frame in the transverse direction. Little information is available on the nature of materials. The walls shown on plan views have been considered as masonry, except the partition walls between classrooms considered as non-structural elements. The roof is a roof terrace.

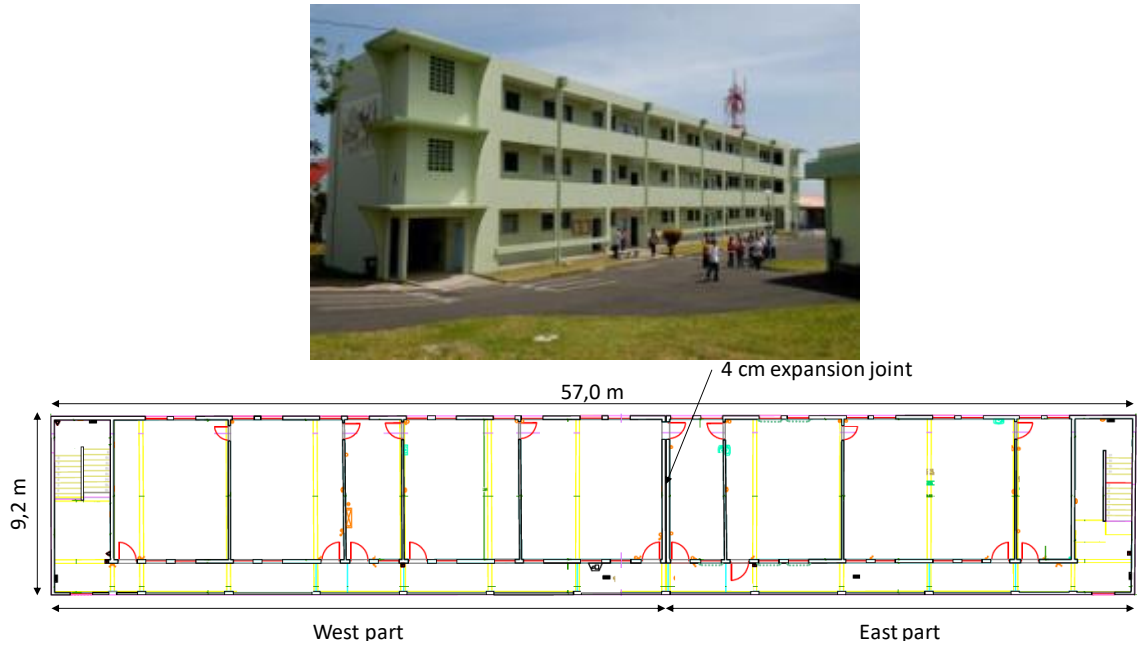

Figure 1. Overview of the building (at the top) and the first floor plan view (at the bottom)

3. EARTHQUAKES AND AMBIENT VIBRATION DATA ANALYSIS

3.1 Instrumentation of CGBP

The building has been instrumented with 24 channels within 12 locations as shown in Figure 2. The instrumentation includes a free-field 3-D sensor at 10 m from the building (n°11), 5 sensors at the base of the building : a 3D sensor (n°0) at the north-west corner, a 3D sensor at the south-east corner (n°3), two channels on both sides of the expansion joint on the transversal direction (n°1 and 2) with a longitudinal channel at location of sensor n°2 and a vertical channel at the north-east corner. Then, at the first floor, two 2-D sensors are available: one at the corner north-west and the other at the south-east corner with channels in the longitudinal and transversal axes of the building (n°5 and 6). Finally, at the third floor 4 locations were instrumented (fixed on the roof inside the building): two at the same place as for the first floor (n° 7 and 10) and two others on both sides of the expansion joint in the transversal direction (n°8 and 9) with a longitudinal component at n°9.
The sensors are Episensor mono-component (ES-U) and Episensor 3-components (EST), those sensors are made by Kinemetrics. All sensors are linked to a same station with 24 channels (Kephren).

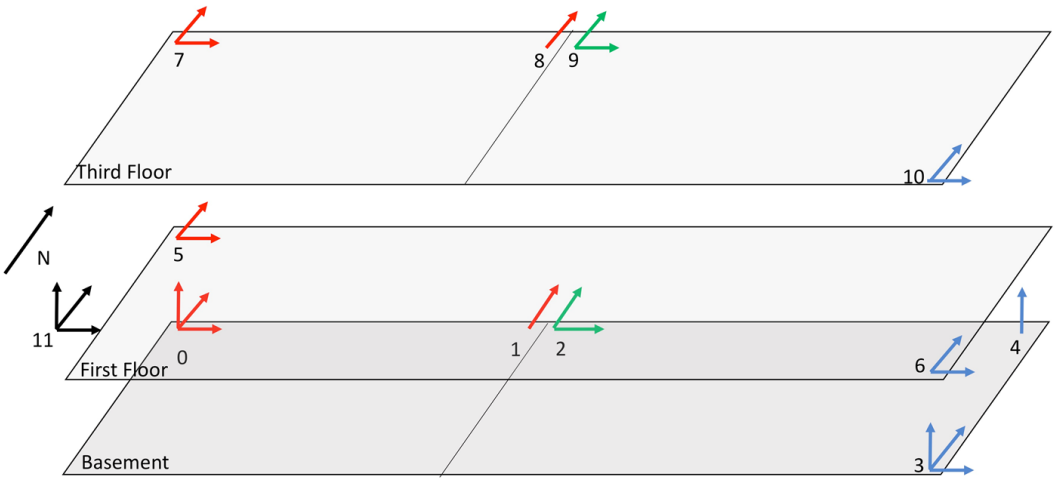

Figure 2. Location of 24 accelerometric channels installed at CGBP building in Martinique French Indies island

3.2 Recorded earthquakes

We used in this study a database that has been prepared by Philippe Gueguen in charge of the RAP/RESIF. The database contains the earthquakes recorded from 2011 to 2014 with a very low maximum PGA up to 0.2 cm/s^2 (Figure 3). These recordings are only weak motions and will be used to understand the dynamic behavior of the building at low strain. The results are therefore comparable with ambient vibrations analysis.

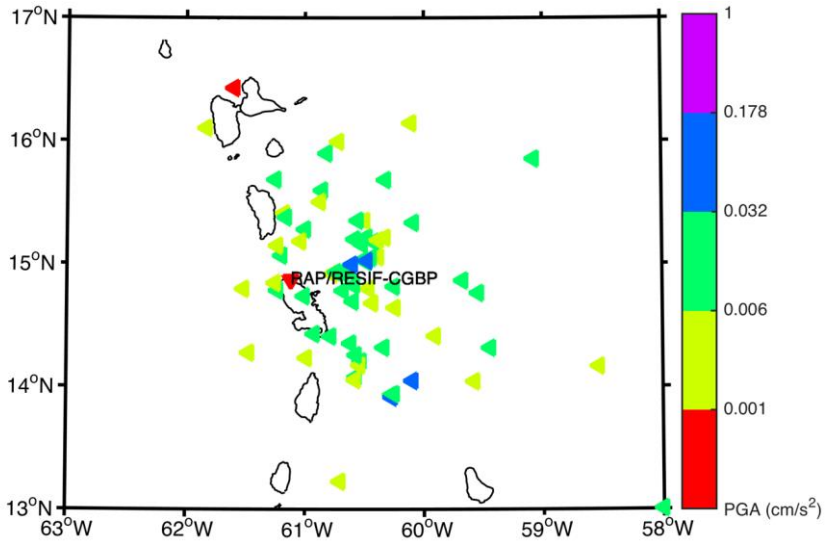

Figure 3. Location of the epicenter of the recorded data according to the maximal PGA (cm/s^2) at CGBP station

4. MODAL IDENTIFICATION USING EARTHQUAKE AND AMBIENT VIBRATIONS DATA

4.1 Calculation of the resonance frequencies of the system (soil-foundation-structure) and subsystems

4.1.1 From earthquake data

If we consider that the system has a linear behavior, the soil-foundation-structure system and parts of it (subsystems) can be characterized with the transfer function between signals recorded at various locations in and outside the building. Let consider a simple model of structure represented by a single

degree-of-freedom oscillator characterized by its height (h), mass (m), stiffness (k), and viscous damping coefficient (c) and resting on a base that can translate and rotate relatively to the soil as illustrated in Figure 4. The motion at the free-field due to an earthquake is called u_g and the motion at the base of the structure will be $u_g + u_f$ with u_f the motion of the base relatively to the soil. The motion at the top of the structure, u_{top}, is composed of three displacements: the motion of the base u_f, the displacement u due to the deformation of the structure and the rocking of the foundation ($u_\theta = h\theta$) as shown in Equation 1.

$$u_{top} = u_g + u_f + h\theta + u \tag{1}$$

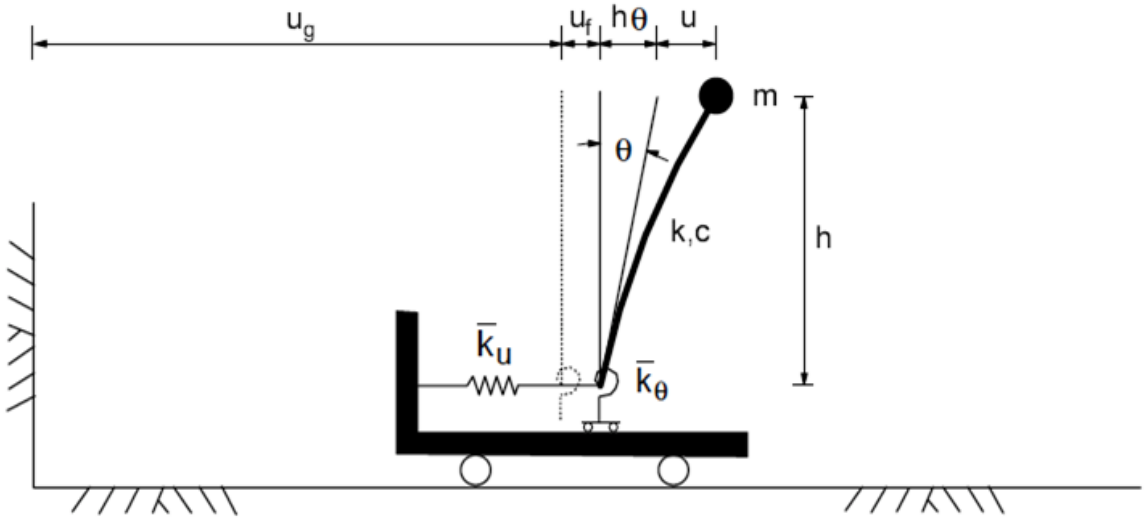

Figure 4. Single degree-of-freedom oscillator representation (from Stewart et Fenves, 1998)

Considering the location of the sensor in the CGBP building, we can access to the frequencies of the soil-foundation-structure system and each subsystem :

- **For the soil-foundation-structure system** : the system frequency called f_{top} is computed with the transfer function between the top (sensor n°7, 9 and 10 in the two horizontal directions and sensor n° 8 for the transversal component) and the free-field (sensor n°11) in several locations in the building.
- **For the soil** : f_{soil} is computed using the horizontal to vertical spectral ratio (e.g. Langston, 1979 ; Lermo et Chavez-Garcia, 1993) of the sensor n°11. However, it is important to note that the soil response could contain part of the energy radiated from the structure, especially when the free-field sensor is close to the structure (Jennings, 1970 ; Gueguen et al., 2000).
- **For the structure** : f_{stru}, is computed by removing from the top recording the rocking displacement and performing the transfer function between top sensors (sensor n°7, 9 and 10 in the two horizontal directions and sensor n° 8 for the transversal component) and base sensors (sensor n°0, 2 and 3 in the two horizontal directions and sensor n° 1 for the transversal component). The rocking motion in the transversal direction is computed using the vertical recordings at sensors n°3 and 4 as illustrated in Equation 2, while the rocking in the longitudinal direction is calculated using sensors n°0 and 4 (Equation 3).

$$h\theta_{trans} \approx h\frac{|u_{z3} - u_{z4}|}{l} \tag{2}$$

$$h\theta_{long} \approx h\frac{|u_{z0} - u_{z4}|}{L} \tag{3}$$

where, h, l and L are the height, the width and the length of the structure respectively. u_{z0}, u_{z3} and u_{z4} are the vertical motion at sensor n°0, 3 and 4 respectively.

Figure 5 illustrates the transfer functions :

- Between the top and the free-field motion for the longitudinal component (a) and the transversal

component (b),

- Between the top and the base motion (u_g + u_f) for the longitudinal component (c) and the transversal component (d),
- Between the top without the rocking motion and the base motion (u_g +u_f) for the longitudinal component (e) and the transversal component (f).

The horizontal to vertical spectral ratio at the free-field sensor is given in Figure 5 (g).

The results are averaged over all recorded earthquakes. The plain lines indicate the average for all earthquakes recorded and the dotted lines represent the ± one standard deviation (considering a lognormal distribution). We chose a similar scale for the amplitude of all subgraphs so the amplitude are comparable.

For the first three types of transfer functions (subgraphs (a, b), (c, d), (e,f)), the spectral ratio at four locations in the building is computed. The curves are represented by different colors : in red in the west part at the north-west corner (that indicates the movement in the stairwell), in green at the west corner but close to the expansion joint at the north-east corner, in blue in the east part close to the expansion joint at the north-west corner and finally in magenta, in the east part at the south-east corner (that indicate the movement in the opposite stairwell).

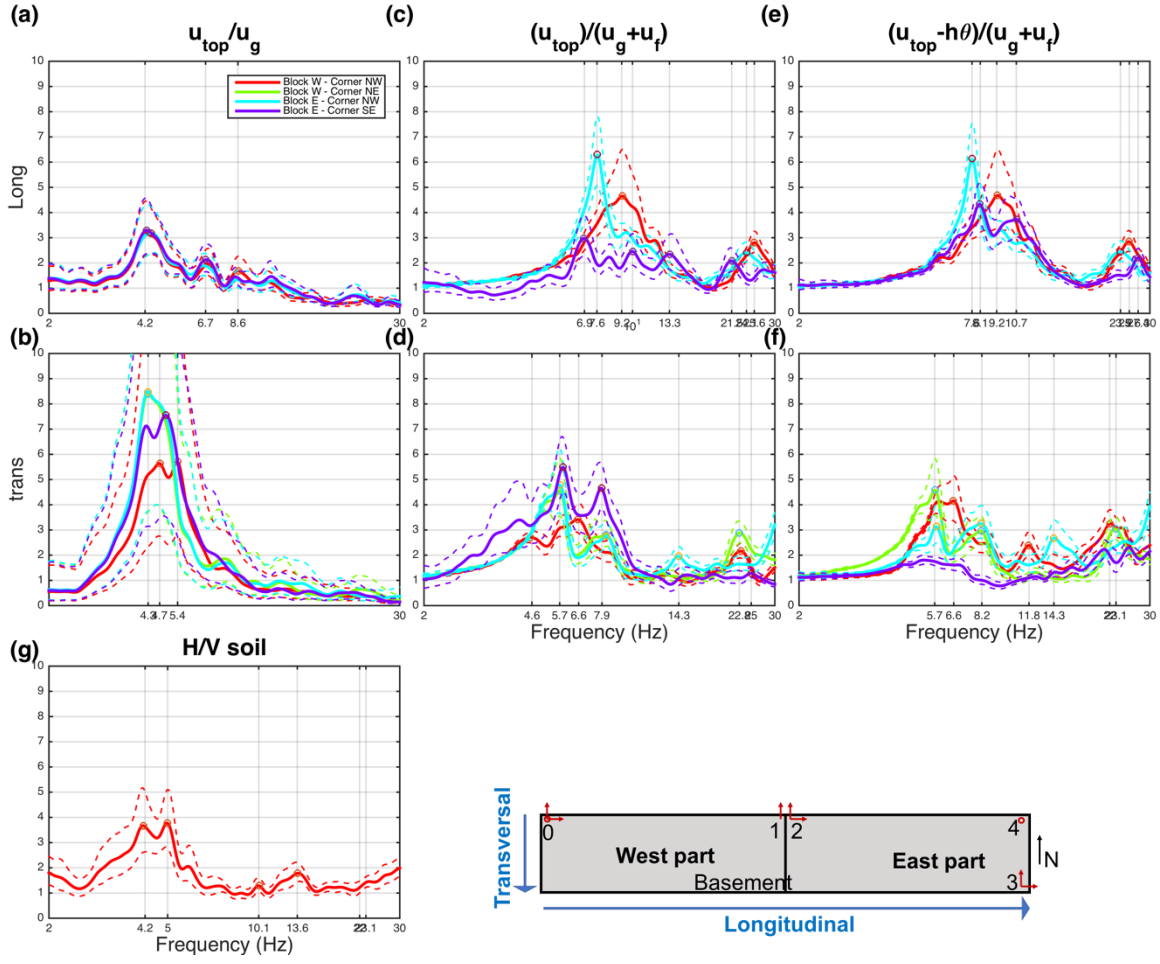

Figure 5. Transfer functions between the top and the free-field motion for the longitudinal component (a) and the transversal component (b), transfer function between the top without the rocking motion and the base motion for (c) the longitudinal component and (d) the transversal and (e) horizontal to vertical spectral ratio at the free-field sensor

From Figure 5, we can deduce that the soil has resonance frequencies closed to 4.2 and 5.0 Hz that can be seen in the H/V ratio (subgraph g). However, the first frequency at 4.2 Hz is seen in the whole soil-foundation-structure response in both directions (subgraphs a and b) and the motion at this frequency

is amplified compared to the ground motion suggesting that this frequency could be link to the foundation-structure system and not to the soil.
Subgraphs (c) and (d) that indicate the resonance frequencies of the structure with rocking motion at the top are not very different from those without rocking motion shown in subgraphs (e) and (f) except at the east stairwell. It shows that the rocking has a different influence on the top motion depending on the location of the sensors in the building and influence only the response of the east stairwell.
Subgraphs (a), (b), (c) and (d) show that the structure is more rigid in the longitudinal axis compared to the transversal axis.
The first longitudinal mode without rocking motion (subgraphs (e) and (f)) is at 7.8 Hz for the east part and 9.2 Hz for the west part. The structure appears to have different behavior in the east and west parts. A secondary frequency at 10.7 Hz is marked on the east part. A series of high frequency modes around 23 Hz are visible and different in the three locations of the building.
In the transversal direction, the transfer functions are also different at different locations in the building. The first transversal modes at 5.7 Hz probably precede by a mode around 4.8 Hz are the only common modes of the whole building, unless less marked in the south-east corner of the east part. On both sides of the expansion joint, the behavior is similar until 12.0 Hz. The peak at 8.2 Hz indicates large movement at the expansion joint and lower at the stairwells which may indicate a torsional mode. The peak at 6.6 Hz is marked on the north-west corner of the west part (stairwell west). Similarly, to the longitudinal component, high frequency modes are present in all location of the building. This first analysis indicates a complex behavior of the structure which is variable from one location to another. The first transversal modes seem to be the only ones common to the whole structure.

4.1.2 From ambient vibration data

A frequency domain decomposition method is also used and applied to the whole recordings except the free-field (e.g. Brincker, Zhang, & Andersen, 2001) based on the codes developed by Keith Soal in his PHD (https://github.com/keithsoal/Frequency-Domain-Decomposition). Figure 6 indicates the first three singular values from the modal decomposition. From this figure, we picked six frequencies at 4.6, 5.6, 7.0, 9.1, 12.8 and 14.4 Hz. The modal shape complexity index provides an evaluation of the phase shifting of the maximal deformation at the measurement points. A frequency that indicates a mode shape of the structure (considering a linear system without rotational component and with hysteretic damping being distributed proportionally in all elements), should provide maxima at the same instant in the all parts of the structure. The value is between 0 (Real Mode) and 1 (Imaginary Mode). The complexity of the corresponding mode shapes lies between 0 and 0.15 except for the last two modes where it is above 0.4 suggesting that these two frequencies may not represents more shape or at least complex ones (with rotational component for instance). Compared to the previous analysis, there is no distinction of directions for each frequency, the mode shape will provide more information. However, we can already observe that the first longitudinal mode around 8 Hz are not seen in the ambient vibrations data.

4.2 Calculation of the mode shape

To complete the first study of the Fourier content of the recordings, an analysis of the mode shapes was performed. We used both earthquake and noise recordings. For the earthquake recordings, the mode shapes were calculated using the relative displacement of each component and sensor location to a reference (sensor and component with the highest amplitude). The displacement was filtered around each presumed modal frequency selected in the previous analysis and average over all earthquakes.
For the noise recordings, the frequency domain decomposition method is used.
In Figure 7 the mode shapes from the earthquake recordings (red line) and ambient vibrations (dashed line) are compared for three frequencies that could correspond to the first transversal and longitudinal mode shapes that were common to both analysis. The mode shapes are normalized and it is important to note that the sensor with maximal amplitude (reference sensor) can be different for both analysis. A linear interpolation between measuring points was performed. In the figure, no axis is represented but the scale for the deformation is similar from one subgraph to another.

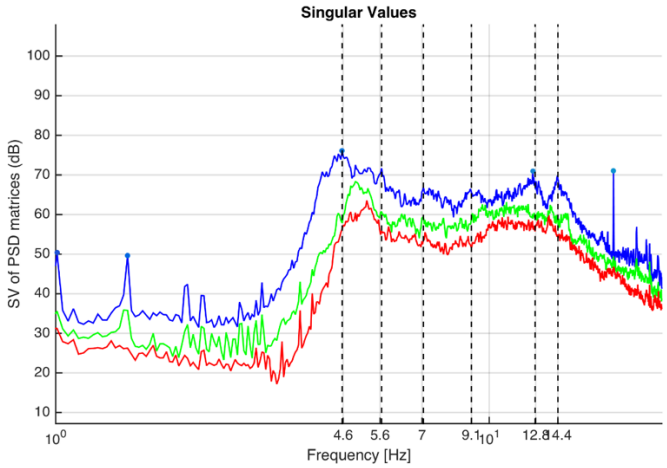

Figure 6. First three singular values coming from the frequency domain decomposition

Green lines and associated numbers in Figure 7 indicate the initial location of sensors. The comparison is made in 1D to facilitate the reading. The four vertical planes containing sensors displacements are shown on the transversal and longitudinal direction. The vertical motion at the base in both directions (vertical lines 0-4 and 3-4) is also shown to observe any foundation rocking.

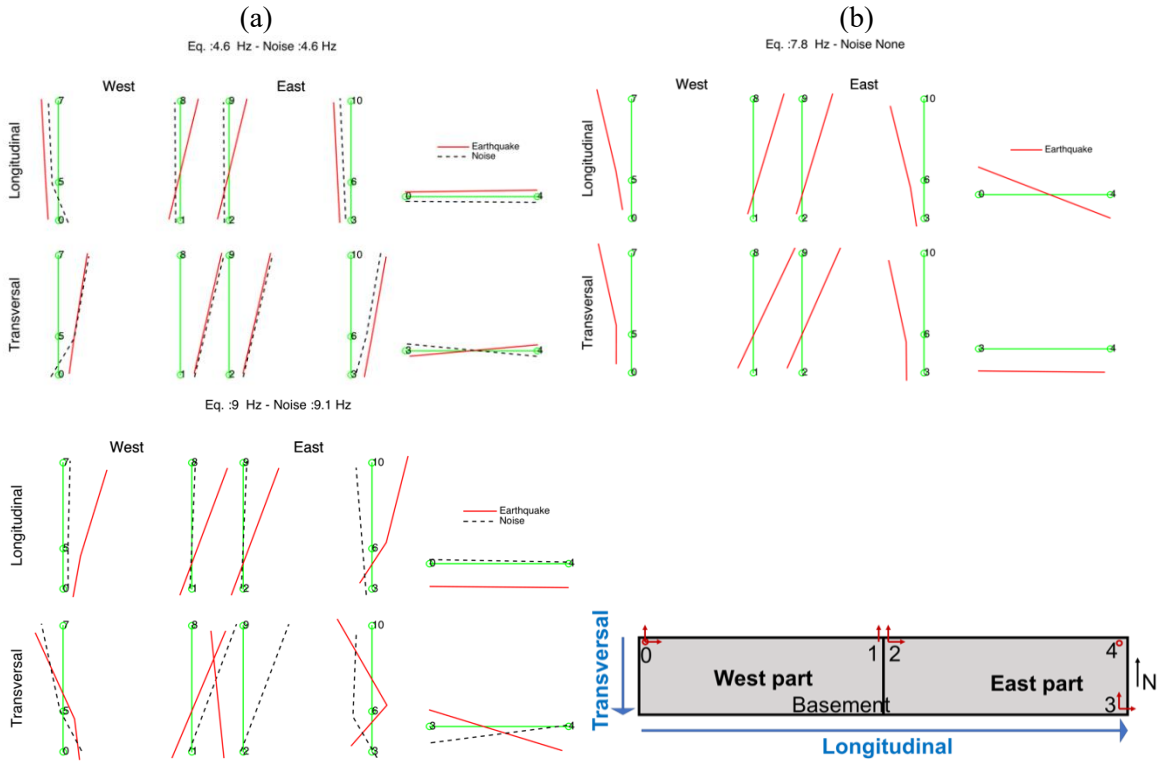

Figure 7. Comparison of the mode shapes computed with earthquake and noise data for the modes at (a) 4.6Hz (b) 7.8Hz and (c) 9Hz.

For the first transversal mode, we chose a frequency of 4.6 Hz and for the longitudinal mode shape we chose 7.8 and 9Hz. The frequency at 7.8Hz is only seen in the earthquake data.

For the first transversal mode (subgraph a), the transversal deformation coming from the earthquakes or noise recordings are very close, especially at the expansion joint where both displacement of the structure and translation of the foundations are similar. The longitudinal deformation is however more pronounced in the earthquake recordings.

The longitudinal mode at 7.8Hz was observed in Figure 5(e) as a peak of the east part of the building

with higher amplitude at the expansion joint. For the west part of the building, the higher peak is at 9.2 Hz but an intermediate peak is visible in Figure 5(e) at 7.8 Hz and is confirmed by the mode shape analysis with important deformations of the west part at this frequency. The behavior of the building at 7.8 Hz is complex: the longitudinal deformation of the expansion joint is in the opposite direction compared to the deformation at the stairwells and we observe a large longitudinal rocking of the base. The deformation is also high in transversal components at this longitudinal mode. Torsion and rocking behavior of the building could be considered at this frequency.
One possible explanation of the discrepancy between the first longitudinal mode found in the earthquake and in the noise recordings, is that earthquake recording trigger a mode shape that noise cannot linked to the rocking of the foundations.
For the mode at 9 Hz (subgraph c), the longitudinal displacement is only seen in the earthquake data, the ambient vibration data indicate a mode shape that appears to be on the transversal component.

All the mode shapes coming from the earthquake and the noise recordings data are compared using the MAC (Modal Assurance Criterion) coefficient that quantify the closeness of the mode shapes. The MAC value can be between 0 and 1. Values larger than 0.9 indicate consistent correspondence whereas small values indicate poor resemblance of the two mode shapes. Figure 8 illustrates the values of the MAC for the transversal, longitudinal and vertical components for each frequency found with earthquake and noise recordings analysis. The transversal mode shapes are close for frequencies below 11.0 Hz at similar modal frequencies (4.4, 5.2, 7.8 and 10.1 Hz). For the longitudinal component, the discrepancy between the mode shapes is much higher the MAC values are low for equivalent frequencies (diagonal terms). For the vertical component, the trend between mode shapes is less clear but a very good agreement is reach for the first mode shape.

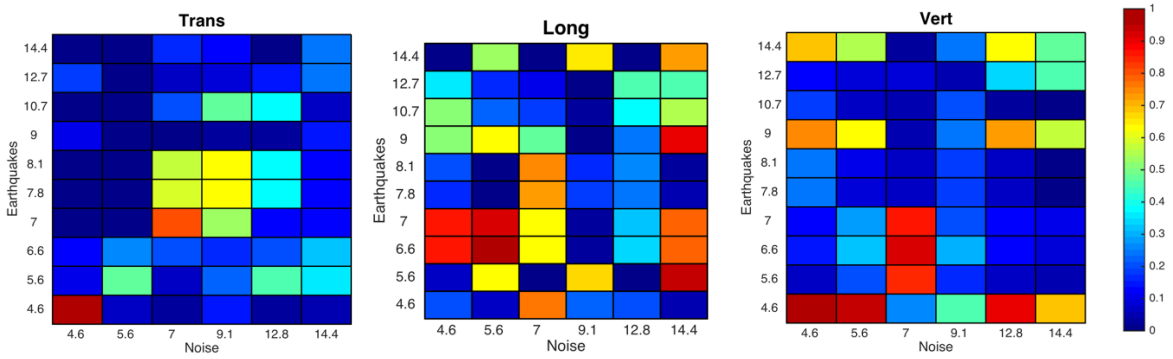

Figure 8. MAC values between mode shapes for each component calculated from earthquakes and noise recordings

5. BUILDING MODEL

This part presents the numerical model of the building and its updating by comparison with earthquake and ambient vibration data.

5.1 Model presentation

A finite element model of the building has been performed by 3D structural modelling implemented in Advance Design (2018). The two parts of the building (east and west) were modeled separately considering the expansion joint to be fully functional (Figure 9).
Soil-structure interaction was ignored in the model to first calibrate structural parameters.
To evaluate the impact of masonry walls on the dynamic characteristics, various models of the building were performed. First, the building was studied with concrete frame only (model A). A second modelling was carried out taking into account the masonry walls that were considered continuous on the entire level (model B). Finally, a third model was evaluated (model C) with additional masonry walls below the openings (windows) and bodyguards. In all models, only partition walls, in the transverse direction, were ignored.

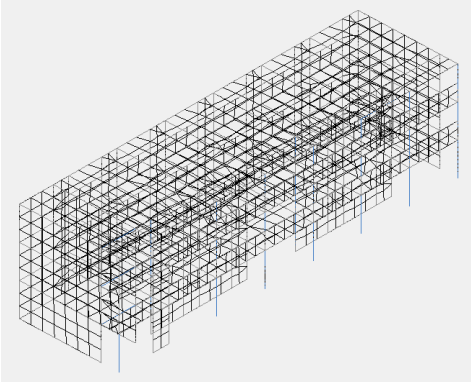

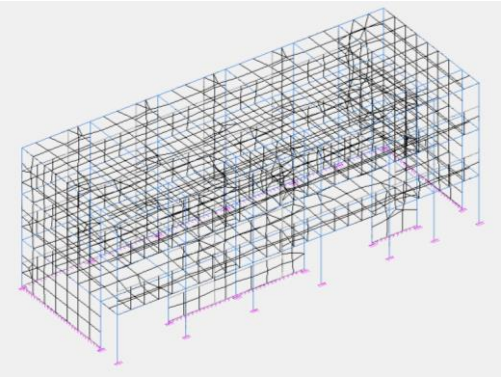

Figure 9. Model of the building : Left : west part of the building (1851 nodes – 204 linear elements – 139 surface elements) – Right : east part of the building (1413 nodes – 156 linear elements – 102 surface elements

5.2 Parametric studies

Different parameters have been tested for the model updating :

- Modulus of elasticity of concrete elements (beams, columns and floor slabs) : the initial value at the construction time (1972) should be more or less 30 000 MPa, depending on the quality of materials and application. However, since 1972 the building suffered from seismic activities that probably lead to cracking in concrete elements, decreasing apparent modulus of elasticity hence the value of 20 000 MPa tested in the parametric study.
- Modulus of elasticity of masonry
- Percentage of live load Q in the combination of weight. Three combinations were tested: the required combination when designing equivalent new building (G+0.24Q from EN 1998-1 §3.2.4 (2)P), a combination without load Q (considering only gravity loads G) and a third combination G+Q.
- Model of masonry walls (model A, B and C presented in §5.1)

The dynamic characteristics compared for this parametric study is the first natural period in both directions.

Table 1. Parameters tested for the parametric study and resulting first periods in both directions for the west part of the building.

	Model of structure	**Modulus of elasticity E of concrete (Mpa)**	**Modulus of elasticity E of masonry (Mpa)**	**Weight combination**	**First frequency (Hz) longitudinal**	**First frequency (Hz) transversal**
1	Model A (*)	20 000	-	G + 0,24 Q	1.4	1.6
2	Model A (*)	20 000	-	**G**	1.4	1.5
3	Model A (*)	20 000	-	**G + Q**	1.3	1.5
4	Model A (*)	**30 000**	-	G + 0,24 Q	1.6	2.0
5	**Model B** (*)	20 000	**1 000**	G + 0,24 Q	2.6	3.3
6	**Model B** (*)	20 000	**10 000**	G + 0,24 Q	5.0	6.8
7	**Model C** (*)	20 000	**10 000**	G + 0,24 Q	8.4	6.8

(*) models are presented in §5.1
Bold type highlights parameters which differ from the reference model (yellow line)

Some results of the parametric study are presented in Table 1 only for the west part of the building.

- Change in live load Q (models 1,2 and 3 in table 1) has little impact on the value of the periods: less than 10% difference between the models with and without live load.
- Adding masonry walls in the model (from model A to model B), even with low modulus of elasticity, make the structure significantly more rigid. Indeed, the natural periods are decreased by half when modeling the masonry walls with a modulus of elasticity of 1 000 MPa in the model B. In this latter model, which considers only the walls continuous on the entire levels, the building is more flexible in the longitudinal direction (period: 0.39s) than in the transversal one (period: 0.30s). The Earthquake and ambient data reveal a different behavior, pointing out that longitudinal rigidity is underestimated in model B. Model C was tested considering in addition walls below windows and bodyguard (all in longitudinal direction) and indicate closer values to the observations in the two directions. These results highlight that the ambient vibration and weak motion data are sensitive to the filling masonry and non-structural elements. In case of stronger motions those elements will not be mobilized during the whole duration and the rigidity should be lower, independently of non-linear behavior of the structure.

The model used to compare the mode shapes in §5.3 is the model n°7. The first frequencies for east and west parts in this configuration are given in Table 2.

Table 2. First periods in both directions for east and west parts of the building.

	First longitudinal frequency (Hz)	**First transversal frequency (Hz)**
West part of the building	8.4	6.8
East part of the building	7.5	7.2

5.3 Comparison with real data

We compared the results from the numerical simulations to the ones obtained from earthquake and noise measurements. Only the first longitudinal and transversal modes are compared. Noise and earthquake data indicate a first transversal mode at 4.6 Hz for both east and west parts. The mode shapes at this frequency are compared in Figure 10(a) to the first transversal modes of the numerical simulation (6.8 Hz for west part and 7.2 Hz for east part).
In the longitudinal direction, we found from the earthquake analysis first modes at 7.8 Hz for the east part and 9.2 Hz for the west part. Such frequencies are not present in the ambient vibration analysis which indicates a first longitudinal frequency at 12.8Hz. Figure 10(b) and (c) represent respectively the mode shapes at 7.8Hz and 12.8Hz.
The mode shapes illustrated in Figure 10 are represented with a linear interpolation between measuring points. All mode shapes are normalized with a reference sensor (sensor with maximal deformation) that can be different for all three analyses (earthquake, noise and numerical analysis). No deformation axis is represented on the figure but the same scale (for the deformation) has been used for all subgraphs.
The first transversal mode (subgraph a) is similar in the transversal direction for the numerical simulation and the observations except for the base motion that is null (fixed base condition) in the numerical model.
In Figure 10 (b), the first longitudinal mode from earthquake analysis (at 7.8Hz) is compared to the first longitudinal modes of the numerical model. The longitudinal displacements are similar at the expansion joint but not at the stairwells and transversal displacement are also larger in the observations compared to the modelling. The numerical model gives a first longitudinal mode with predominant longitudinal deformation whereas the first longitudinal mode from the earthquake analysis is associated to a torsion and rocking behavior of the structure.
For the longitudinal mode at 9Hz (subgraph c), the longitudinal deformations are close especially to the ones obtained from earthquake data at the expansion joint.

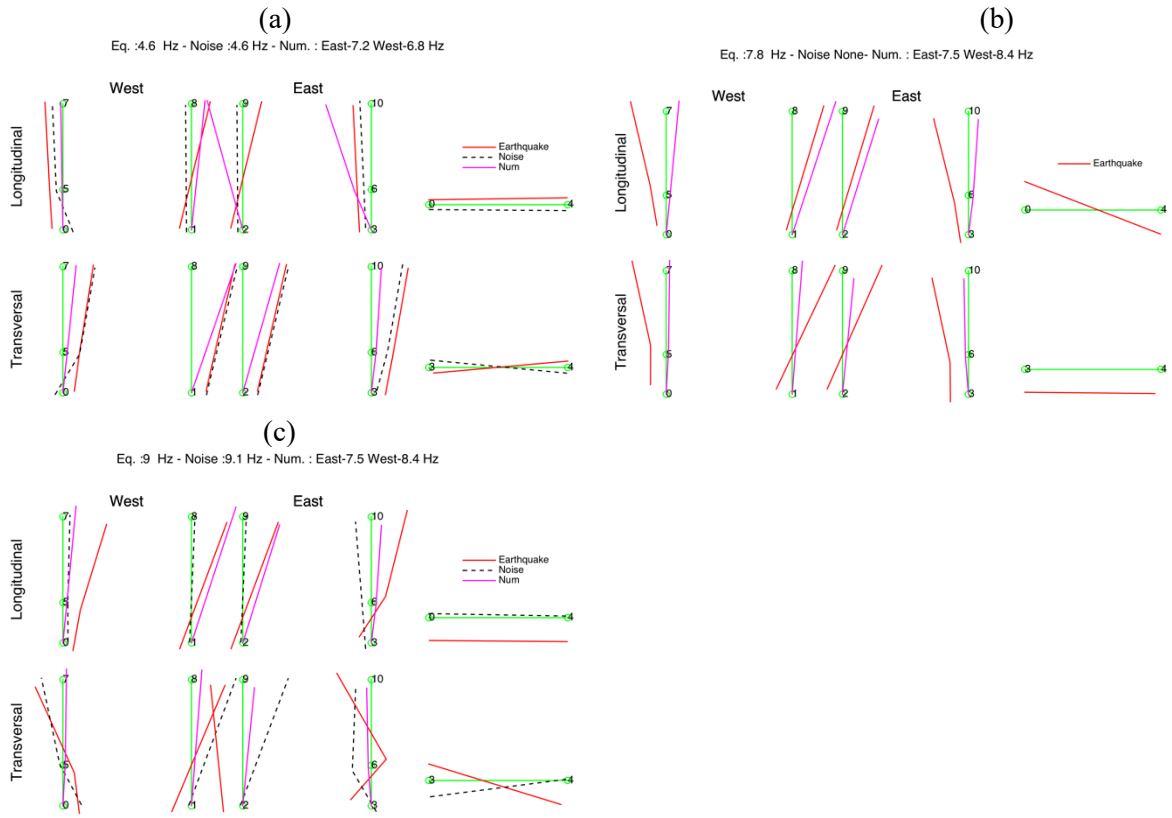

Figure 10. Comparison of the mode shapes calculated with earthquake, noise data and numerical simulation for the modes: (a) first transversal mode at 4.6Hz, (b) longitudinal mode at 7.8 Hz and (c) longitudinal mode at 9 Hz

6. DISCUSSIONS AND CONCLUSIONS

The behavior of the high school in Basse-Pointe is complex, with different behavior of the east and west parts of the building. The earthquake and noise recordings data provide close results even if the frequencies of the first longitudinal mode are different. The earthquake recordings provide frequencies close to 8.0 Hz that are not seen in the ambient vibration recordings. It is possible that earthquake trigger modes that cannot be seen by ambient vibrations and especially rocking of the foundation. Such observations have been also shown in (Lorenzo Fernández ,2016) with the prefecture building of Nice for which the expansion joint of the structure was not participating to the dynamic response of the structure.

A more detailed measurement setup, at least for a non-permanent acquisition of ambient vibrations recordings would have improve the characterization of the mode shapes of the structure. For example, some intermediate sensors between the corners in both east and west parts of the building in three directions would have help precise if one mode was a torsion of the whole structure or a deformation of only one part.

The numerical simulation provides closer results to the observations when adding all non-structural elements to the model (model C). The modellings and the observations provide mode shapes for the first transversal and longitudinal modes close to the observations in the main direction of deformation and at the expansion joint. Nevertheless, the frequencies of the modes differ between the modelling and the observations. The modelling was performed considering that east and west part of the building are completely separated, and this assumption could change the longitudinal rigidity of the structure which can explain part of the discrepancies observed. Besides, the soil-structure interaction was not initially considering in the modelling. These two drawbacks of the modelling are the main topics of our current work.

6. ACKNOWLEDGMENTS

The authors are grateful to the RESIF/RAP who founded this project and provide the accelerometric and ambient vibrations that were used in this article.

7. REFERENCES

Brincker R., L. Zhang, P. Andersen (2001), Modal identification of output-only systems using Frequency Domain Decomposition, Smart Mater. Struct. 10:441-445.

Chandra, J. (2014). Nonlinear seismic response of the soil-structure system: experimental analyses. Université Grenoble Alpes.

Chávez-García, F. J., & Bard, P.-Y. (1994). Site effects in Mexico City eight years after the September 1985 Michoacan earthquakes. Soil Dynamics and Earthquake Engineering, 13(4), 229–247.

Fernández Lorenzo, G. W., Mercerat, D., Santisi D'Avila, M. P., Bertrand, E., & Deschamps, A. (2015). Operational Modal Analysis of a high rise RC building and modelling. In The 6th International Operational Modal Analysis Conference. Gijón, Spain.

Gueguen, P., Bard, P. Y., & Oliveira, C. S. (2000). Experimental and numerical analysis of soil motions caused by free vibrations of a building model. Bulletin of the Seismological Society of America, 90(6), 1464–1479.

Gueguen, P., Michel, C., & LeCorre, L. (2007). A simplified approach for vulnerability assessment in moderate-to-low seismic hazard regions: application to Grenoble (France). Bulletin of Earthquake Engineering, 5, 467–490.

Jennings, P. C. (1970). DISTANT MOTIONS FROM A BUILDING VIBRATION TEST. *Bulletin of the Seismological Society of America*, *60*(6), 2037–2043.

Lorenzo Fernández, guillermo. (2016). Des données accélérométriques au comportement dynamique des bâtiments existants. Côte d'Azur.

Luco, J. E., Trifunac, M. D., & Wong, H. L. (1988). Isolation of soil-structure interaction effects by full-scale forced vibration tests. Earthquake Engineering & Structural Dynamics, 16(1), 1–21.

Michel, C., Guéguen, P., & Bard, P.-Y. (2008). Dynamic parameters of structures extracted from ambient vibration measurements: An aid for the seismic vulnerability assessment of existing buildings in moderate seismic hazard regions. Soil Dynamics and Earthquake Engineering, 28(8), 593–604.

Stewart, J. P., & Fenves, G. L. (1998). System identification for evaluating soil–structure interaction effects in buildings from strong motion recordings. Earthquake Engineering & Structural Dynamics, 27(8), 869–885.

Todorovska, M. I. (2009a). Separation of the Effects of Soil-Structure Interaction in Frequency Estimation of Buildings From Earthquake Records. In Coupled Site and Soil-Structure Interaction Effects with Application to Seismic Risk Mitigation (pp. 169–178). Springer. Retrieved from http://link.springer.com/chapter/10.1007/978-90-481-2697-2_13

Todorovska, M. I. (2009b). Soil-Structure System Identification of Millikan Library North-South Response during Four Earthquakes (1970-2002): What Caused the Observed Wandering of the System Frequencies? Bulletin of the Seismological Society of America, 99(2A), 626–635. https://doi.org/10.1785/0120080333